Solar Energy Materials & Solar Cells 147 (2016) 108–114

Contents lists available at ScienceDirect

Solar Energy Materials & Solar Cells

journal homepage: www.elsevier.com/locate/solmat

Generalised distributed model of a solar cell: Lateral injection effects and impact on cell design and characterisation

Dongchen Lan*, Martin A. Green

Australian Centre for Advanced Photovoltaics, School of Photovoltaic and Renewable Energy Engineering, University of New South Wales, Sydney 2052, Australia

ARTICLE INFO

Article history:
Received 20 October 2015
Received in revised form
30 November 2015
Accepted 11 December 2015

Keywords:
Solar cell modelling
Solar cell equivalent circuit

ABSTRACT

Increasing insights into the operational features of experimental solar cells, particularly the effects of spatial variations arising from material quality fluctuations or device design features, are being made possible by advanced characterisation technologies, such as luminescent imaging. A widely used two-dimensional model of solar cells underpinning the interpretation of such effects consists of a network of distributed elemental solar cells connected by resistive elements. This model is refined to account rigorously for lateral carrier and photon flows in the cell bulk by incorporation of a network of pseudo-current sources. An example of the use of the new model is given by analysing the lateral injection effect due to voltage variation along the emitter under operating conditions. The derived results not only provide a more general insight into such a lateral injection mechanism, but also reveal the impact on luminescent imaging.

1. Introduction

In characterizing multidimensional effects in solar cells, as increasingly important in luminescent imaging [1–5], the simple model of independent diodes is commonly used. A more sophisticated model is the resistively coupled, distributed diode model of Fig. 1 [6], which takes horizontal balancing currents into account [7]. This model applies to the normal situation such as for the majority of commercial cells where a p–n junction extends over the top surface of the device. In the most general case, all elements are spatially dependent. Using the enormous range of information that can be generated by techniques such as luminescent imaging under different bias and illumination conditions, values can be determined for the spatial distribution of these elements. In the most refined cases, parameters such as the ideality factor components of the diode saturation currents [3], local generation currents and local voltages and resistances [4] can be determined and plotted in a manner that facilitates rapid diagnostics.

A limitation of this model is that it does not account for the lateral diffusive flow of carriers in the cell bulk. This introduces a fundamental inconsistency between modelled and experimental devices that can cause misinterpretation of the cell parameters extracted in this way. A recent work [8] showed that lateral carrier diffusion due to material non-uniformity can affect photoluminescence images of silicon wafers. Similarly, an impact can be anticipated on luminescence images of solar cells in addition too the effects due to non-uniform voltage distribution discussed in the present work. In the present work, it is shown that the lateral diffusive effects can be rigorously incorporated as pseudo-photogeneration sources, allowing the commonly used distributed model to be simply generalised to include these effects. An example of how the new model can be used is then given by comprehensive analysis of lateral injection effects due to voltage variation along the emitter, including the impact on luminescence measurements.

2. Basic theory for modelling lateral non-uniformity

2.1. Pseudo-1D equation

Assuming low level injection, a very general formulation of the device properties in a region of given polarity at steady state is [9–11]:

$$-\nabla\left[D(\boldsymbol{r})p_0(\boldsymbol{r})\nabla u(\boldsymbol{r})\right]+\frac{p_0(\boldsymbol{r})u(\boldsymbol{r})}{\tau(\boldsymbol{r})}=G(\boldsymbol{r})+\int_V \kappa(\boldsymbol{r},\boldsymbol{r}')u(\boldsymbol{r}')dV' \quad (1)$$

where $p(\boldsymbol{r})$ is the actual minority carrier density, $p_0(\boldsymbol{r})$ is its value in thermal equilibrium, $u(\boldsymbol{r})=\left[p(\boldsymbol{r})-p_0(\boldsymbol{r})\right]/p_0(\boldsymbol{r})$ is the normalised excess minority carrier density, $D(\boldsymbol{r})$ and $\tau(\boldsymbol{r})$ are the minority carrier diffusivity and lifetime, respectively, $G(\boldsymbol{r})$ is the generation rate due to external illumination, whereas the term on the far right accommodates photon recycling with $\kappa(\boldsymbol{r},\boldsymbol{r}')$ being the equilibrium

* Corresponding author.
E-mail address: d.lan@unsw.edu.au (D. Lan).

http://dx.doi.org/10.1016/j.solmat.2015.12.005
0927-0248/

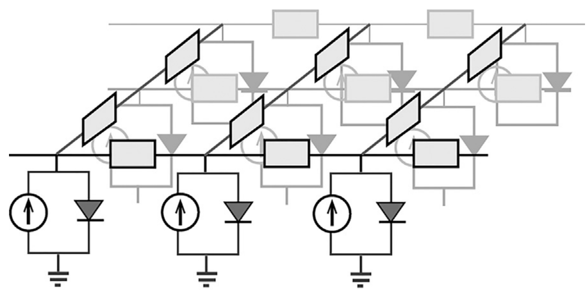

Fig. 1. Widely used approximate distributed model of a solar cell. Parasitic shunt elements can be added if required (after Ref. [6]).

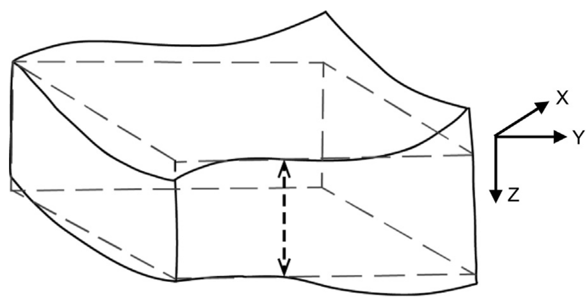

Fig. 2. Example of a general solar cell domain V (solid lines) and an equivalent 1D domain V_1 (dashed lines).

generation rate at $\boldsymbol{r}$ due to photon emission at $\boldsymbol{r}'$ as specified elsewhere [10, 11].

Expressing in terms of spatial coordinates (x, y, z) at a particular spatial location (x_1, y_1) as shown by the dashed arrow in Fig. 2 and rearranging the result give:

$$-\frac{\partial}{\partial z}\left[D(x_1,y_1,z)p_0(x_1,y_1,z)\frac{\partial u(x_1,y_1,z)}{\partial z}\right]+\frac{p_0(x_1,y_1,z)u(x_1,y_1,z)}{\tau(x_1,y_1,z)}$$
$$=G(x_1,y_1,z)+G_{ps}(x_1,y_1,z)$$
$$+\int_{V_1}\kappa\left[(x_1,y_1,z),\ (x',y',z')\right]u(x',y',z')dx'dy'dz', \quad (2)$$

where the group of terms on the right hand side (RHS) of the equation is hereafter referred to as the *effective generation rate*. Here,

$$G_{ps}(x_1,y_1,z)=\frac{\partial}{\partial x}\left(D(\boldsymbol{r})p_0(\boldsymbol{r})\frac{\partial u(\boldsymbol{r})}{\partial x}\right)\bigg|_{x_1,y_1}+\frac{\partial}{\partial y}\left(D(\boldsymbol{r})p_0(\boldsymbol{r})\frac{\partial u(\boldsymbol{r})}{\partial y}\right)\bigg|_{x_1,y_1}$$
$$+\left\{\int_V\kappa\left[(x_1,y_1,z),\ (x',y',z')\right]u(x',y',z')dx'dy'dz'\right.$$
$$\left.-\int_{V_1}\kappa\left[(x_1,y_1,z),\ (x',y',z')\right]u(x',y',z')dx'dy'dz'\right\} \quad (3)$$

$G_{ps}(x_1,y_1,z)$ is termed as pseudo-photogeneration source. The integrations involved are over the actual domain V of interest (solid lines of Fig. 2) or a constructed equivalent 1D domain V_1 (dashed lines of Fig. 2).

From the mathematical perspective, at each (x, y) coordinate, Eq. (2) is identical to the 1-D equation in the z-variable that would apply in a uniform device shown by the dashed line construction in Fig. 2, with the effects of spatial variation with x and y fully incorporated by a modification of the generation term. The corresponding equivalent circuit is shown in Fig. 3. The effect of lateral non-uniformities is simply incorporated into the solar cell equivalent circuit by the addition of an extra current source at each node. While determining the value of this pseudo-current source is not trivial in general, the evaluation of the other elements is straightforward. They are given by the value at each location (x_1, y_1) that would be deduced for a uniform device with the properties at the line (x_1, y_1, z) throughout.

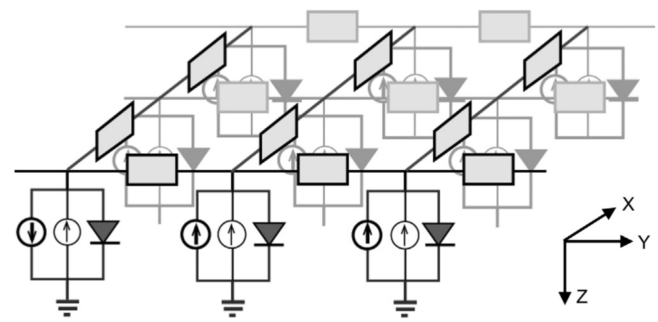

Fig. 3. More accurate distributed model of a solar cell including the additional pseudo-current sources shown in bold.

The new circuit model accommodates spatial variations in all parameters, but the following analysis underpinning the model relies on the normal assumption of low level injection and injection level independent device properties as specified in more detail elsewhere [9], in which case Eqs. (1) and (2) are linear.

2.2. Dark/light reciprocal relationship

The advantage of the pseudo-1D form of Eq. (2) is that the solution for the "pseudo-dark" case (zero effective generation) is readily found. Although not the actual dark solution where device properties are a function of (x, y), the pseudo-dark solution can be used to find the collection probability of photogenerated carriers, $f_C(\boldsymbol{r})$, by a non-intuitive link between the latter and the dark minority carrier distribution first identified by Donolato [12]. This reciprocal relationship has been extended to very general 3D geometries by Green [9] and further extended to include photon recycling [10,11]. With this determinable $f_C(\boldsymbol{r})$, the value of the additional current sources in Fig. 3 at the (x_1, y_1) coordinate of interest can be identified as:

$$J_{ps}(x_1,y_1)=q\int f_C(x_1,y_1,z)\ G_{ps}(x_1,y_1,z)dz, \quad (4)$$

while those of the standard current sources can be similarly given by:

$$J_{LG}(x_1,y_1)=q\int f_C(x_1,y_1,z)[G(x_1,y_1,z)$$
$$\left[+\int_{V_1}\kappa\left[(x_1,y_1,z),\ (x',y',z')\right]u(x',y',z')dx'dy'dz'\right]dz. \quad (5)$$

In situations where the photon recycling effects are negligible, $f_C(\boldsymbol{r})$ can be found analytically when the material properties are uniform in the z-direction [13]. [Analytical solutions are also known for a range of other possible z-axis variations including those involving built-in fields with corresponding spatial variations in carrier lifetime [14].] Neglecting the photon recycling term, under steady illumination, J_{LG} is independent of changes in operating conditions, while J_{ps} can be. This corresponds to the introduction of an injection level dependent term into the formulation.

The generalised circuit and dark/light reciprocal relationship noted above are valuable in analysis of lateral injection effects as shown in subsequent sections.